BCS-BEC crossover and quantum phase transition for ^{6}Li and ^{40}K atoms across the Feshbach resonance

W. Yi and L.-M. Duan
FOCUS center and MCTP, Department of Physics, University of Michigan, Ann Arbor, Michigan 48109, USA
(Received 22 March 2006; published 6 June 2006)

We systematically study the BCS-BEC crossover and the quantum phase transition in ultracold ^{6}Li and ^{40}K atoms across a wide Feshbach resonance. The background scattering lengths for ^{6}Li and ^{40}K have opposite signs, which lead to very different behaviors for these two types of atoms. For ^{40}K, both the two-body and the many-body calculations show that the system always has two branches of solutions: one corresponds to a deeply bound molecule state; and the other, the one accessed by the current experiments, corresponds to a weakly bound state with population always dominantly in the open channel. For ^{6}Li, there is only a unique solution with the standard crossover from the weakly bound Cooper pairs to the deeply bound molecules as one sweeps the magnetic field through the crossover region. Because of this difference, for the experimentally accessible state of ^{40}K, there is a quantum phase transition at zero temperature from the superfluid to the normal Fermi gas at the positive detuning of the magnetic field where the *s*-wave scattering length passes its zero point. For ^{6}Li, however, the system changes continuously across the zero point of the scattering length. For both types of atoms, we also give a detailed comparison between the results from the two-channel and the single-channel model over the whole region of the magnetic field detuning.

DOI: 10.1103/PhysRevA.73.063607 PACS number(s): 03.75.Ss, 05.30.Fk, 34.50.−s

I. INTRODUCTION

Ever since the experimental observation of the condensation of fermion pairs in dilute gases of ultracold fermionic atoms, the study of the BCS-BEC crossover in ultracold fermionic gases has attracted much attention [1,2]. The crossover in ultracold fermion gases is facilitated experimentally by the Feshbach resonance, where the interatomic interaction can be tuned over a large range by varying the external magnetic field [3]. Various experiments have been done recently in ultracold fermionic gases in the vicinity of the Feshbach resonance to study the properties of the BCS-BEC crossover [1].

In most experiments, either an equal mixture of ^{40}K atoms in the $|F=9/2, m_F=-9/2\rangle$ and the $|F=9/2, m_F=-7/2\rangle$ hyperfine states or an equal mixture of ^{6}Li atoms in the $|F=1/2, m_F=-1/2\rangle$ and the $|F=1/2, m_F=1/2\rangle$ states are prepared and magnetically tuned across a wide Feshbach resonance ($B_0=202$ G for ^{40}K and $B_0=834$ G for ^{6}Li). Because of the nature of the wide resonance, for both atom species, their properties close to the resonance point are very similar [4–6]. However, they indeed have an important difference that is not quite emphasized before: the background scattering lengths for ^{40}K and ^{6}Li have opposite signs. This sign difference in the background scattering has profound effects when the system is outside the unitary region.

In this paper, we investigate the different properties of ^{40}K and ^{6}Li atoms arising from their distinction in the background scattering. To describe the Feshbach resonance, we use the standard two-channel model that is characterized by three parameters determined from the scattering data: the resonance width, the detuning, and the background scattering length [2,5,7]. The main differences between ^{40}K and ^{6}Li are summarized as follows: First, for the ^{40}K atoms, there always exist two stable solutions to the many-body gap and number equations; while for the ^{6}Li atoms, there is only one solution. The current experiments with ^{40}K atoms probe only one branch of the solution through the adiabatic sweep. For this experimentally relevant branch, the closed channel population is always limited to a small fraction, no matter how far the magnetic field is detuned. This unusual property of ^{40}K has been noted before, in association with a somewhat different model Hamiltonian that is characterized by five experimental parameters [8,9]. For future experiments with ^{40}K, there might also be the possibility to switch to the other branch of the solution through a fast sweep, if the three-body collision does not turn out to be a significant obstacle to the stability of such a state (note that the three-body collision is not taken into account in the two-channel Hamiltonian). Second, a probably more interesting difference is that there exists a quantum phase transition at zero temperature for the ^{40}K atoms; while there is no such transition for ^{6}Li. Note that here we limit ourselves to the case with equal populations for the two spin components, where there is no phase transition in the standard BCS-BEC crossover theory. Nevertheless, for the experimentally accessible branch of solution of the ^{40}K atoms, due to the effect of the background scattering in the two-channel model, a quantum phase transition from the superfluid state to the normal Fermi gas occurs on the BCS side of the resonance, basically around the point where the scattering length goes across zero. For the ^{6}Li atoms, however, when the scattering length crosses the zero point, which is on the BEC side, the change in the state of the system is completely continuous.

In this work, we have also systematically compared the results from the two-channel model and from the single-channel model over the whole region of the magnetic field detuning (from the far negative to the far positive). The standard single-channel model is characterized by only a single parameter, the scattering length at the corresponding field detuning. Our results extend some of the comparisons in Refs. [4] to the off-resonance region, with particular empha-

sis on the effects arising from the difference in the background scattering of the two atom species. For easier comprehension of the properties of the many-body solutions, we also present the solutions for the two-body states with the same model Hamiltonian for comparison. The paper is arranged as follows: In Sec. II, we present the model Hamiltonians, and discuss their two-body states for ^{6}Li and ^{40}K atoms. Then, in Sec. III, we apply the two channel and the single channel models, respectively, to study the many-body properties of the ultracold atoms at zero temperature. The properties calculated include the energy gap, the chemical potential, and the closed channel population. In Sec. IV we analyze in detail the quantum phase transition for the ^{40}K atoms on the BCS side. Finally, in Sec. V, we discuss the finite temperature behavior, and calculate the critical temperatures and the pseudogaps corresponding to the different branches of solutions for ^{6}Li and ^{40}K atoms. For this finite-temperature calculation, we follow the G_0G method as reviewed in Ref. [5] to include the pair fluctuations. The results are summarized in Sec. VI.

II. THE MODEL HAMILTONIANS AND THEIR TWO-BODY STATES

The Feshbach resonance in ultracold atoms can be understood on the grounds of two colliding fermions in different hyperfine states. In dilute ultracold gases, the interaction can be described by the s-wave atomic scattering. The magnetic field tunes the interaction strength by Zeeman shifting the energy level of the quasibound state (the Feshbach molecule state) relative to the continuum threshold of free atoms. The physics is well described by the following two-channel model [2,7]:

$$\begin{aligned} H = & \sum_{\sigma,\mathbf{k}} \epsilon_{\mathbf{k}} a^{\dagger}_{\mathbf{k},\sigma} a_{\mathbf{k},\sigma} + \sum_{\mathbf{q}} (\gamma + \epsilon_{\mathbf{q}}/\mathbf{2}) b^{\dagger}_{\mathbf{q}} b_{\mathbf{q}} \\ & + (U/\mathcal{V}) \sum_{\mathbf{k},\mathbf{k}',\mathbf{q}} a^{\dagger}_{\mathbf{k}+\mathbf{q}/2,\uparrow} a^{\dagger}_{-\mathbf{k}-\mathbf{q}/2,\downarrow} a_{-\mathbf{k}'-\mathbf{q}/2,\downarrow} a_{\mathbf{k}'+\mathbf{q}/2,\uparrow} \\ & + (g/\sqrt{\mathcal{V}}) \sum_{\mathbf{k},\mathbf{q}} (b^{\dagger}_{\mathbf{q}} a_{-\mathbf{k}+\mathbf{q}/2,\downarrow} a_{\mathbf{k}-\mathbf{q}/2,\uparrow} + \text{H.c.}), \end{aligned} \tag{1}$$

where $a^{\dagger}_{\mathbf{k},\sigma}$ and $b^{\dagger}_{\mathbf{q}}$ are the creation operators for the open channel fermions (the atoms) and the closed channel bosons (the molecules), respectively; $\epsilon_{\mathbf{k}} = \hbar^2 k^2/(2m)$ (m is the atom mass); $\mathcal{V}$ is the quantization volume, and $\sigma = \uparrow, \downarrow$ denotes the different hyperfine states of the atoms. This Hamiltonian is characterized by three parameters: the bare atom-molecule coupling rate g, the bare background atom scattering rate U, and the bare detuning γ. These three bare quantities are connected with the physical ones g_p, U_p, γ_p through the standard renormalization relations: $U = \Gamma U_p$, $g = \Gamma g_p$, $\gamma = \gamma_p - \Gamma g_p^2/U_c$, where $\Gamma \equiv (1 + U_p/U_c)^{-1}$ and $U_c^{-1} \equiv -\Sigma_{\mathbf{k}}(1/2\epsilon_{\mathbf{k}})$ [5]. The physical quantities g_p, U_p, γ_p are determined from the scattering data as $U_p = 4\pi\hbar^2 a_{bg}/m$, $g_p^2 = 4\pi\hbar^2 a_{bg} \Delta B \mu_{co}/m$, and $\gamma_p = \mu_{co}(B - B_0)$ (μ_{co} is the difference in magnetic moments between the two channels) [10], where we have assumed that the s-wave scattering length near resonance has the form $a_s = a_{bg}[1 - \Delta B/(B - B_0)]$, with a_{bg} as the background scattering length, ΔB as the resonance width, and B_0 as the resonance point.

If the population in the closed channel is negligible, one can adiabatically eliminate the molecular modes $b_{\mathbf{q}}$ in the Hamiltonian (1), and arrive at the following simplified single-channel model:

$$\begin{aligned} H = & \sum_{\sigma,\mathbf{k}} \epsilon_{\mathbf{k}} a^{\dagger}_{\mathbf{k},\sigma} a_{\mathbf{k},\sigma} \\ & + (U^{eff}/\mathcal{V}) \sum_{\mathbf{k},\mathbf{k}',\mathbf{q}} a^{\dagger}_{\mathbf{k}+\mathbf{q}/2,\uparrow} a^{\dagger}_{-\mathbf{k}-\mathbf{q}/2,\downarrow} a_{-\mathbf{k}'-\mathbf{q}/2,\downarrow} a_{\mathbf{k}'+\mathbf{q}/2,\uparrow}, \end{aligned} \tag{2}$$

where U^{eff} is connected with the physical one U_p^{eff} by the renormalization relation $U^{eff} = U_p^{eff}(1 + U_p^{eff}/U_c)^{-1}$, and U_p^{eff} is determined solely by the scattering length a_s as $U_p^{eff} = 4\pi\hbar^2 a_s/m$ at the corresponding magnetic field detuning. So, a single-channel model does not explicitly depend on the resonance width or the background scattering rate, it only depends on their combination through the expression of a_s. In this sense, a single-channel model is simpler and more universal. However, given a new configuration, we typically do not know whether the closed channel population is negligible prior to the calculation, therefore the validity of the single-channel model is not self-evident. We will have some systematic comparison of the results from the two-channel and the single-channel calculations for ^{40}K and ^{6}Li over the whole region of the magnetic field detuning. A similar comparison has been done before in the unitary region [4,5], where the background scattering can be neglected.

To have some intuitive understandings of the Hamiltonian above, we first look at its bound states for two particles. For a two-channel model, the eigenstate of the Hamiltonian in the case of two particles can be written as the superposition of the molecular bosons in the closed channel and the fermion pairs in the open channel,

$$|\Psi\rangle = \sum_{\mathbf{k}} c_{\mathbf{k}} a^{\dagger}_{\mathbf{k},\uparrow} a^{\dagger}_{-\mathbf{k},\downarrow} + c_b b^{\dagger}_0 |0\rangle, \tag{3}$$

where $c_{\mathbf{k}}$ and c_b are the superposition coefficients, and we have assumed that the center-of-mass momentum $\mathbf{q} = \mathbf{0}$ as it is decoupled from the relative momentum in the two-body case. The Schrödinger's equation $H|\Psi\rangle = E|\Psi\rangle$ then gives

$$\begin{aligned} \frac{1}{U_p - \dfrac{g_p^2}{\gamma_p - E}} &= -\frac{1}{\mathcal{V}} \sum_{\mathbf{k}} \left(\frac{1}{2\epsilon_{\mathbf{k}} - E} - \frac{1}{2\epsilon_{\mathbf{k}}} \right) \\ &= 2^{-7/2} \pi^{-1} \left(\frac{\hbar^2}{2m} \right)^{-3/2} \sqrt{-E}, \end{aligned} \tag{4}$$

where we have used the renormalization relation $1/[U_p - g_p^2/\gamma_p] = 1/[U - g^2/\gamma] + (1/\mathcal{V})\Sigma_{\mathbf{k}}[1/(2\epsilon_{\mathbf{k}})]$.

We solve the bound state energy levels of ^{6}Li and ^{40}K, respectively. The parameters for the ^{6}Li atoms are $a_{bg} = -1405 a_0$, $\Delta B = -300$ G, and $\mu_{co} \sim 2\mu_B$, where a_0 is the Bohr radius and μ_B is the Bohr magnetic moment. The parameters for the ^{40}K atoms are $a_{bg} = 174 a_0$, $\Delta B_0 = 7.8$ G, and $\mu_{co} \sim 1.68\mu_B$. The results of our calculation are plotted in

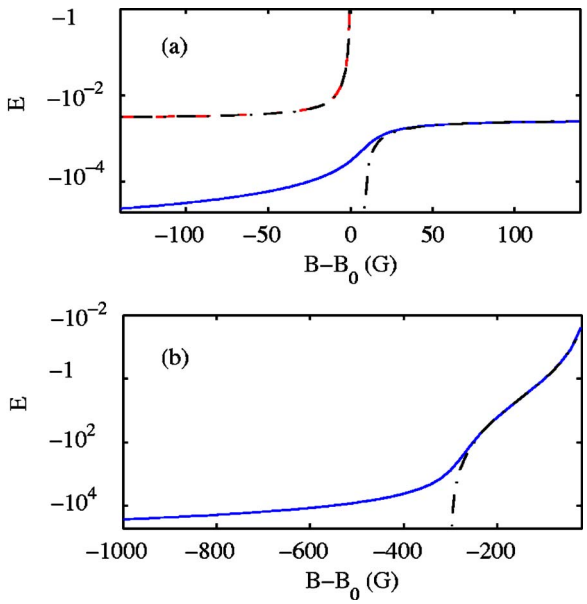

FIG. 1. (Color online) The bound state energy levels for two colliding atoms of (a) ^{40}K, (b) ^{6}Li. The solid curves are the deeply bound states, the dashed curve is the weakly bound state in ^{40}K, and the dash-dotted curves are the results from the single-channel Hamiltonian. To compare with the many-body calculations that follow, the unit of energy is taken to be $E_F=\hbar^2(3\pi^2 n)^{2/3}/2m$, where the total particle densities (n) are chosen to be typical values in the experiments ($n\sim 1.8\times 10^{13}$ cm^{-3} for ^{40}K, and $n\sim 2.9\times 10^{13}$ cm^{-3} for ^{6}Li [1]).

Fig. 1. The outstanding feature of the figures is that there are two branches of bound state for ^{40}K [Fig. 1(a)]. One branch is a deep-bound molecule state that never crosses the continuum threshold (zero energy in the plots). In this state, the closed channel fraction ($|c_b|^2$) becomes dominant as one approaches the negative detuning. The other branch (the upper one) is a weakly bound pair state that crosses the continuum threshold at $\gamma=0$. In this state, the closed channel fraction is always limited to a small fraction ($<6\%$), no matter how much the magnetic field is detuned. In experiments, one approaches the bound state by adiabatically tuning the magnetic field, starting from the atom continuum. Therefore the branch of state with weakly bound pairs is the one accessed in the current experiments. If one wants to go to the deeply bound molecule state, one either needs a fast magnetic field sweep with a rate larger than the energy splitting between the two bound states, or use some rf pulses to couple these two branches. For the ^{6}Li atoms, in contrast, there is only one branch of solution, which merges into the continuum at $\gamma=0$ and approaches the deep-bound molecule state as one increases the negative field detuning. This difference between the two atom species comes from the different natures of their background scattering interactions. For ^{40}K with a positive background scattering length, as has been discussed in Refs. [8,9,11] (the Hamiltonians therein are characterized by five parameters and are somewhat different from the model here), there is a weakly bound state in the open collision channel. The avoided level crossing between this weakly bound state and the Feshbach molecule level gives the two branches of solutions. For ^{6}Li with a negative background scattering length, there is no bound state in the open channel, and thus there is only a single branch of solution.

For comparison, we have also calculated the two-body bound states using the single channel Hamiltonian (2). In the single-channel approach, one simply replaces $U_p-g_p^2/(\gamma_p-E)$ in Eq. (4) with U_p^{eff}, so the left side of Eq. (4) becomes energy independent. Equation (4) then gives the well known expression of the bound energy $E=-\hbar^2/(ma_s^2)$ in the region $a_s\geqslant 0$ for the single-channel mode. The results of the calculation are shown as the dash-dotted curves in Fig. 1. The single channel calculation gives almost the same bound state energies for the weakly bound state of ^{40}K atoms (it neglects the other branch of solution); while it deviates from the results of the two channel calculation as the atomic scattering length a_s approaches its zero point (corresponding to $B-B_0=7.8$ G for ^{40}K, and $B-B_0=-300$ G for ^{6}Li).

III. THE MANY-BODY STATES

To find out the many-body state at zero temperature, one needs to minimize the energy corresponding to the Hamiltonian (1) under the constraint of total particle number conservation $N\equiv\Sigma_{\sigma,\mathbf{k}}a^\dagger_{\mathbf{k},\sigma}a_{\mathbf{k},\sigma}+2\Sigma_{\mathbf{q}}b^\dagger_{\mathbf{q}}b_{\mathbf{q}}$. One therefore minimizes $\Omega=\langle H-\mu N\rangle$, where μ is the Lagrange multiplier with the physical meaning of the chemical potential. We follow the standard BCS-BEC crossover theory [12], which assumes a mean field for the molecule and the pair operators, with $\langle b_{\mathbf{q}}\rangle=\langle b_0\rangle\delta_{\mathbf{q}0}=-(g/\sqrt{\mathcal{V}})\Sigma_{\mathbf{k}}\langle a_{-\mathbf{k},\downarrow}a_{\mathbf{k},\uparrow}\rangle/(\gamma-2\mu)$, where the second equality comes from the Heisenberg equation for the operator $b_{\mathbf{q}}$. Under such an assumption, one can find out the explicit expression of the energy Ω, whose extrema conditions $\partial\Omega/\partial\langle b_0\rangle=\partial\Omega/\partial\mu=0$ yield the standard gap equation and the number equation:

$$\frac{1}{U_p-g_p^2/(\gamma_p-2\mu)}=-\frac{1}{\mathcal{V}}\sum_{\mathbf{k}}\left(\frac{1}{2E_{\mathbf{k}}}-\frac{1}{2\epsilon_{\mathbf{k}}}\right), \tag{5}$$

$$n_{tot}=2n_b+\frac{1}{\mathcal{V}}\sum_{\mathbf{k}}\left(1-\frac{\epsilon_{\mathbf{k}}-\mu}{E_{\mathbf{k}}}\right), \tag{6}$$

where the quasiparticle excitation energy $E_{\mathbf{k}}=\sqrt{(\epsilon_{\mathbf{k}}-\mu)^2+|\Delta|^2}$, and the gap $\Delta=g\langle b_0\rangle/\sqrt{\mathcal{V}}+(U/\mathcal{V})\Sigma_{\mathbf{k}}\langle a_{-\mathbf{k},\downarrow}a_{\mathbf{k},\uparrow}\rangle=z_b\langle b_0\rangle/\sqrt{\mathcal{V}}$ [$z_b\equiv g-U(\gamma-2\mu)/g=g_p-U_p(\gamma_p-2\mu)/g_p$]. In Eq. (6), n_{tot} denotes the total particle density, and $n_b=|\langle b_0\rangle|^2/\mathcal{V}$ is the density of the closed channel molecules.

With Eqs. (5) and (6), we can solve for the gap, the chemical potential, and the closed channel fraction at different magnetic field detunings. The results of the calculations for ^{40}K and for ^{6}Li are plotted in Fig. 2 and Fig. 3, respectively. For ^{40}K, similar to the two-body case, Eqs. (5) and (6) support two branches of solutions. The properties of the first branch of solutions is shown in Figs. 2(a)–2(c). Compared with the results in the previous section, it is easy to see that this solution corresponds to the deep-bound state in the two-body energy spectrum. The closed channel fraction increases from 0 in the BCS limit to 1 in the BEC limit, and the

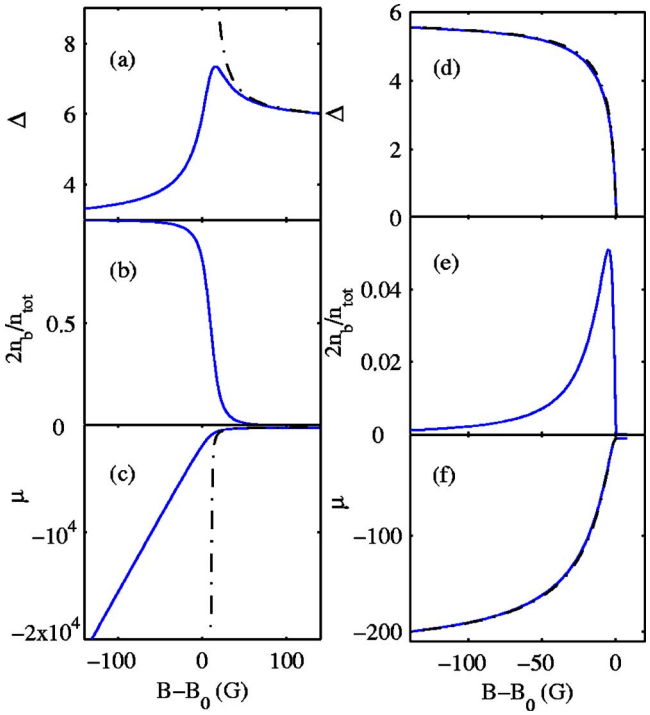

FIG. 2. (Color online) Results from the many-body calculation for ^{40}K atoms at zero temperature. (a)–(c) The gap, the closed channel fraction, and the chemical potential of the solution that corresponds to the deeply bound state in the two-body case; (d)–(f) the gap, the closed channel fraction, and the chemical potential of the solution that corresponds to the weakly bound state in the two-body case. The solid curves are the results using two-channel Hamiltonian. The dash-dotted curves are the results using single channel Hamiltonian. The unit of energy is the same as defined in the caption of Fig. 1.

maximum in the gap appears on the BCS side of the resonance, near the $a_s=0$ point. As the chemical potential always remains negative for this branch, the system is essentially BEC-like at all magnetic field detunings. The properties of the second branch of solution is shown in Figs. 2(d)–2(f), where the closed channel fraction is nonmonotonic, peaks around $B-B_0\sim-5.2$ G with a fraction $\sim5.1\%$, in rough agreement with the calculations in Refs. [8,9], where a different model is used. The chemical potential in this branch crosses zero on the BEC side of the resonance, demonstrating the existence of a BCS-BEC crossover for this branch. The most intriguing feature of the second branch is that there is a quantum phase transition on the BCS side of the resonance, beyond which the superfluid disappears, and the system phase transits into a normal Fermi gas. We will discuss this phase transition in more detail in the next section. The properties of ^{6}Li atoms are shown in Fig. 3. The closed channel fraction remains small throughout the crossover region, and only becomes appreciable deep in the BEC region. The peak in the gap occurs again near the $a_s=0$ point (now on the BEC side). The chemical potential crosses zero around $B-B_0\sim-85$ G, denoting a BCS-BEC crossover.

For comparison, we have calculated the gap and the chemical potential using the single channel Hamiltonian. For the single-channel approach, one just replaces $U_p-g_p^2/(\gamma_p-2\mu)$ with U_p^{eff} in the gap equation (5) and drops the closed channel population contribution $2n_b$ in the number equation (6). The results are shown in Fig. 2 and Fig. 3 in dash-dotted curves. The results from the single channel calculation should coincide with the two channel calculation provided that the closed channel population is small. From Fig. 2 and Fig. 3, it is obvious that, except for the deep-bound state solution of ^{40}K, the single channel Hamiltonian reproduces the results of the two channel Hamiltonian for ^{40}K and ^{6}Li for most of the crossover region. Notably, the single channel description is a fairly good approximation for almost all magnetic field detunings for the weakly bound state solution of ^{40}K, as the closed channel fraction in this branch remains small. In both cases, the single channel description breaks down near the point where $a_s=0$.

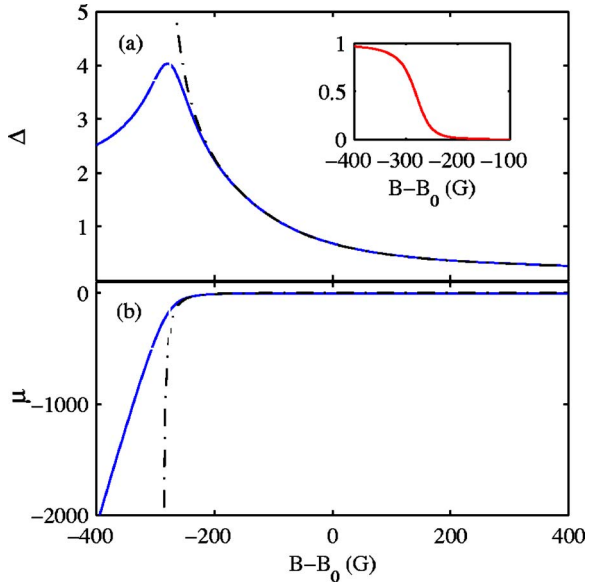

FIG. 3. (Color online) Results from the many-body calculation for ^{6}Li atoms at zero temperature. (a) The gap and the closed channel fraction (inset); (b) The chemical potential. The solid curves are the results using two-channel Hamiltonian. The dash-dotted curves are the results using single channel Hamiltonian.

IV. QUANTUM PHASE TRANSITION FOR ^{40}K ATOMS

To see more clearly the quantum phase transition, we plot the gap and the closed channel fraction from the two channel calculation near the phase transition point on a logarithmic scale in Fig. 4. Both the gap and the closed channel fraction show a precipitous drop at the magnetic detuning $B-B_0\sim7.8$ G, the point where $a_s=0$. Beyond that point, the gap equation and the number equation do not have solutions (for the upper branch). This is a clear signature of a quantum phase transition. The ground state of the ^{40}K atoms changes from a BCS superfluid state into a normal state with the gap $\Delta=0$ through a second order phase transition. In contrast, for ^{6}Li atoms (Fig. 3), there is just a smooth crossover for both the gap and the closed channel population at the point where $a_s=0$ ($B-B_0=-300$ G).

The origin of the phase transition comes from the repulsive background interatomic interaction between the ^{40}K at-

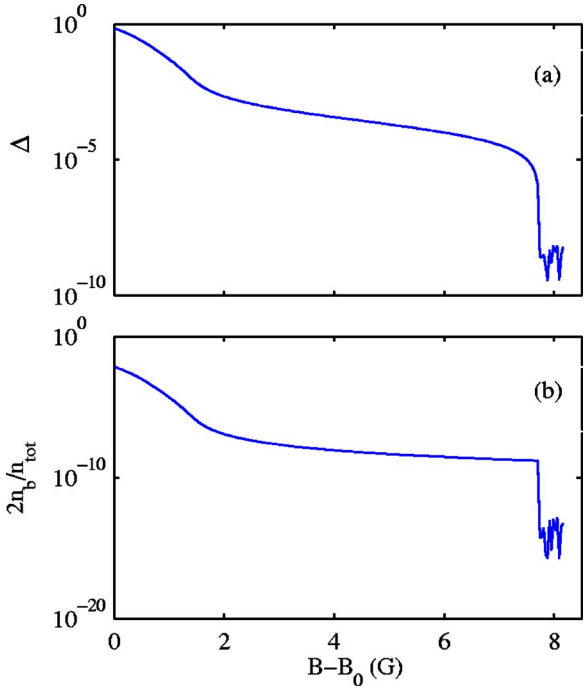

FIG. 4. (Color online) The enlarged (a) gap and (b) closed channel fraction as a function of magnetic field detuning for ^{40}K atoms near the phase transition ($B-B_0\sim 7.8$ G) (corresponding to the weakly bound branch of solution).

oms in the two different hyperfine states. The repulsive interaction does not support a superfluid state that can be adiabatically connected to the BCS superfluid in the region $a_s<0$ (although the system indeed has a superfluid solution corresponding to the deep-bound state, it is not adiabatically connected). So, across the point $a_s=0$, there must be a phase transition, and the atoms transit into a normal phase when $a_s>0$. If one starts from this normal Fermi gas, as the magnetic field decreases toward the resonance ($B_0=202$ G), the atoms will first undergo a second order phase transition and become a BCS superfluid at $B-B_0\sim 7.8$ G. If the field continues to decrease, the chemical potential will eventually become negative at $B-B_0\sim -0.34$ G, and the atoms enter the BEC region with a smooth crossover.

V. THE CRITICAL TEMPERATURES FOR DIFFERENT BOUND STATES

To characterize the crossover properties of different bound states for a different atom species, we calculate the critical temperature at which all the pairs become noncondensed. At finite temperature T, instead of the energy minimization, one needs to minimize the thermodynamical potential $\Omega=-T\ln[\mathrm{tr}(e^{-H/T})]$. If one takes the mean-field approach outlined in Sec. II from the extrema conditions $\partial\Omega/\partial\langle b_0\rangle=\partial\Omega/\partial\mu=0$, one gets the following finite-temperature version of the gap equation and the number equation [2,13],

$$\frac{1}{U_p-\dfrac{g_p^2}{\gamma_p-2\mu}}=-\frac{1}{\mathcal{V}}\sum_{\mathbf{k}}\left(\frac{1-2f(E_{\mathbf{k}})}{2E_{\mathbf{k}}}-\frac{1}{2\epsilon_{\mathbf{k}}}\right), \tag{7}$$

$$n_{tot}=2n_b+\frac{1}{\mathcal{V}}\sum_{\mathbf{k}}\left(1-\frac{\epsilon_{\mathbf{k}}-\mu}{E_{\mathbf{k}}}+2\frac{\epsilon_{\mathbf{k}}-\mu}{E_{\mathbf{k}}}f(E_{\mathbf{k}})\right), \tag{8}$$

where $f(x)=1/(e^{x/k_BT}+1)$ is the Fermi distribution, and k_B is the Boltzmann constant.

This simple mean-field approach, however, is not adequate for the calculation of the critical temperature, except in the case of the BCS limit. The reason is that at finite T, due to the thermal fluctuations, there exist noncondensed pairs (the superposition of fermion pairs and noncondensed bosons), in addition to the condensed fermion pairs and the condensed molecular bosons [5,12]. The noncondensed pairs also contribute to the gap for the fermionic excitations. Accommodating this contribution, the gap is replaced by the total gap $|\Delta|^2=|\Delta_s|^2+|\Delta_{pg}|^2$, where $\Delta_s=z_b\langle b_0\rangle/\sqrt{\mathcal{V}}$ is the same as the gap defined in the previous section (the superfluid order parameter), and the pseudogap Δ_{pg} comes from the contributions of the noncondensed pairs [5,12]. With this simple replacement, the previous gap equation and the number equation from the mean-field approach remain valid. One just needs to interpret Δ as the total gap, and thus the emergence of Δ does not correspond to the critical transition between the normal and the superfluid phase. Instead, the gap shows up at a temperature T^*, below which the noncondensed pairs are formed. As one further decreases the temperature, these preformed pairs finally condense and become a superfluid at the critical temperature T_c with $T_c<T^*$. The gap at the critical temperature T_c solely comes from the pseudogap Δ_{pg}, contributed by the noncondensed pairs (as $\Delta_s=0$ at that point). To calculate this phase transition temperature T_c, one needs to break up the total gap Δ into the superfluid order parameter Δ_s and the pseudogap Δ_{pg}, which requires knowledge of the dispersion relation of the pair excitations. As shown in Ref. [5], the dispersion relation for the pair excitations is still quadratic, with a self-consistently determined effective mass M^*. With that formalism, we calculate the critical temperature T_c and the pseudogap at T_c for different branches of states in ^{40}K and ^{6}Li over the whole region of the magnetic field detuning [13].

The results of the calculation are plotted in Fig. 5 for ^{40}K atoms, and in Fig. 6 for ^{6}Li atoms. Figures 5(a) and 5(b) correspond to the deeply bound state, and Figs. 5(c) and 5(d) correspond to the case with a weakly bound state. It is clear from the T_c calculation that the BCS-BEC crossover picture is evident only for the second branch of the solution [Figs. 5(c) and 5(d)]. For this branch, the critical temperature becomes exponentially small on the BCS side and almost constant on the BEC side, as one expects. For the other branch of the solution corresponding to the deep-bound state, the critical temperature only varies in a very small range, and converges to a constant value on either side of the resonance. One can also see that except in the BCS limit, the pseudogap is still significant at the critical temperature.

VI. SUMMARY

We have systematically studied the BCS-BEC crossover and the quantum phase transition in ultracold ^{6}Li and ^{40}K atoms across a wide Feshbach resonance. As the background

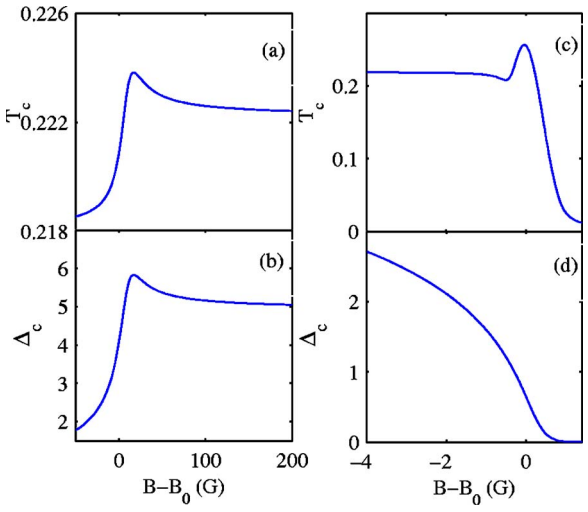

FIG. 5. (Color online) The critical temperature T_c and the pseudogap at the critical temperature Δ_c as a function of magnetic field detuning for the two solutions in ^{40}K atoms [(a), (b) correspond to the deeply bound branch, while (c), (d) correspond to the weakly bound branch]. T_c is in units of T_F, the Fermi temperature associated with the Fermi energy defined in the caption of Fig. 1.

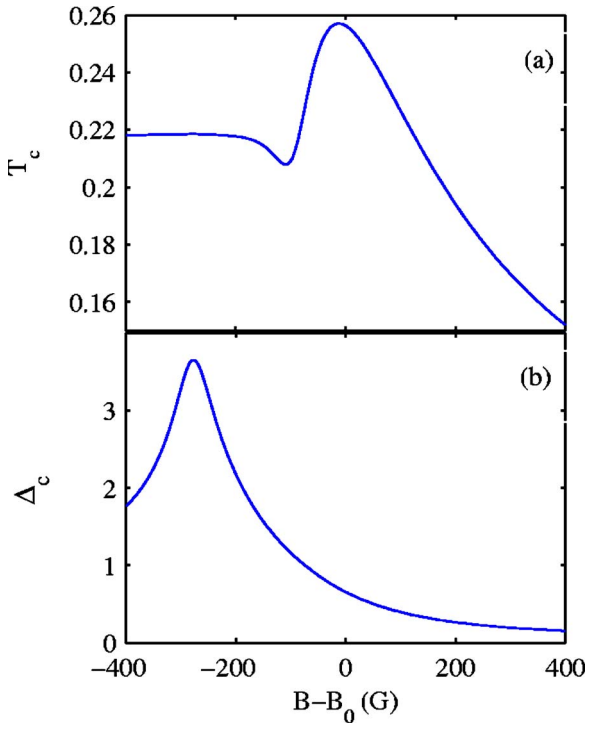

FIG. 6. (Color online) The critical temperature T_c and the pseudogap at the critical temperature Δ_c as a function of magnetic field detuning in ^{6}Li atoms. T_c is in units of T_F, the Fermi temperature associated with the Fermi energy defined in the caption of Fig. 1.

scattering lengths have opposite signs for these two types of atoms, their properties are quite different outside of the near resonance region. Both the two-body and the many-body calculations show that for ^{40}K, there always exist two branches of solutions, corresponding, respectively, to the deep-bound state and the weakly bound states. The latter one with weakly bound pairs is the branch that is accessed by the current experiments through adiabatic sweep. For this branch of solution, there is a quantum phase transition on the BCS side of the resonance, where the atoms phase transit from the superfluid state to the normal Fermi gas as the scattering length crosses zero. This kind of phase transition is absent in the ^{6}Li atoms, where the change in the state of the system is completely continuous when the scattering length goes across its zero point.

The calculations here emphasize the importance of the background scattering length outside the near-resonance region, and the different properties of the ^{6}Li and ^{40}K atoms. In this sense, ^{6}Li and ^{40}K are good representatives of two kinds of atoms that have different background scattering properties. The calculations here may also have some interesting experimental indications. For instance, one can verify the quantum phase transition for the ^{40}K atoms on the BCS side of the resonance, and the continuous crossover for the ^{6}Li atoms on the BEC side of the resonance, although in both cases the scattering length crosses its zero point in a similar way. For the ^{40}K atoms, there might also be the possibility to access the deeply bound branch of solution in future experiments through either a fast magnetic field sweep or some rf transitions.

This work was supported by the NSF awards (0431476), the ARDA under ARO contracts, and by the A. P. Sloan Foundation. We thank Qijin Chen for helpful discussions.

[1] C. A. Regal, M. Greiner, and D. S. Jin, Phys. Rev. Lett. **92**, 040403 (2004); M. W. Zwierlein, C. A. Stan, C. H. Schunck, S. M. F. Raupach, A. J. Kerman, and W. Ketterle, *ibid.* **92**, 120403 (2004); C. Chin *et al.*, Science **305**, 1128 (2004); J. Kinast *et al.*, *ibid.* **307**, 1296 (2005); G. B. Patridge, K. E. Strecker, R. I. Kamar, M. W. Jack, and R. G. Hulet, Phys. Rev. Lett. **95**, 020404 (2005); M. W. Zwierlein *et al.*, Nature **435**, 1047 (2005).

[2] M. Holland, S. J. J. M. F. Kokkelmans, M. L. Chiofalo, and R. Walser, Phys. Rev. Lett. **87**, 120406 (2001); Y. Ohashi and A. Griffin, *ibid.* **89**, 130402 (2002).

[3] R. A. Duine and H. T. C. Stoof, Phys. Rep. **396**, 115 (2004).

[4] R. B. Diener and T.-L. Ho, e-print cond-mat/0405174 (2004); e-print cond-mat/0404517.

[5] Q. J. Chen, J. Stajic, S. Tan, and K. Levin, Phys. Rep. **412**, 1 (2005); Q. Chen and K. Levin, Phys. Rev. Lett. **95**, 260406 (2005).

[6] S. De Palo, M. L. Chiofalo, M. J. Holland, and S. J. J. M. F. Kokkelmans, e-print cond-mat/0404672; D. S. Petrov *et al.*, e-print cond-mat/0502010.

[7] E. Timmermans *et al.*, Phys. Rep. **315**, 199 (1999).
[8] M. H. Szymanska, K. Goral, T. Kohler, and K. Burnett, Phys. Rev. A **72**, 013610 (2005).
[9] N. Nygaard, B. I. Scheider, and P. S. Julienne, e-print cond-mat/0601542, 2006.
[10] L.-M. Duan, Phys. Rev. Lett. **95**, 243202 (2005).
[11] P. D. Drummond and K. V. Kheruntsyan, Phys. Rev. A **70**, 033609 (2004).
[12] D. M. Eagles, Phys. Rev. **186**, 456 (1969); A. J. Leggett, in *Modern Trends in the Theory of Condensed Matter* (Springer-Verlag, Berlin, 1980), pp. 13–27; P. Nozières and S. Schmitt-Rink, J. Low Temp. Phys. **59**, 195 (1985).
[13] W. Yi, L.-M. Duan, Phys. Rev. A **73**, 031604(R) (2006).